

# CRN Application to Predict the NO<sub>x</sub> Emissions for Industrial Combustion Chamber

Nguyen Thanh Hao<sup>1</sup> and Park Jungkyu<sup>2</sup>

<sup>1</sup>Industrial University of HoChiMinh City, 12, NguyenVanBao, GoVap, HoChiMinh, Vietnam

<sup>2</sup>Department of Mechanical Engineering, Konkuk University, 120 Neungdong, Gwangjin, Seoul, Korea

Email: [nguyenthanhhao@hui.edu.vn](mailto:nguyenthanhhao@hui.edu.vn)

(Received on 15 March 2013 and accepted on 15 May 2013)

**Abstract** – The development of chemical reactor network (CRN) models to predict the NO<sub>x</sub> emissions is very important for the modern combustion system design. In this study, the new chemical reactor network models are constructed based on the computational fluid dynamics (CFD) to simulate the burning process of the industrial combustor. The boundary and the operating conditions used for these CRN models reflect the typical operating conditions of the industrial combustor. The global mechanism has been developed by GRI 3.0 in the UW chemical reactor code. For the reliability of the predictive models, the models were analyzed and compared to the experimental industrial combustor research. Finally, the CRN models have shown to be efficient estimating accurately NO<sub>x</sub> emissions with a very short response time.

**Keywords:** Industrial Combustion Chamber, NO<sub>x</sub> Emissions, Chemical Reactor Networks (CRN), Computational Fluid Dynamics (CFD)

## I. INTRODUCTION

Controlling the remaining pollutant emission is one of the most important design goal in developing combustion system. Detailed knowledge of NO<sub>x</sub> formation in the flame is required for the ultra-low NO<sub>x</sub> lean premixed combustors. Relatively small changes in the system boundary conditions can lead to a large emission increase. Therefore, the modeling of the combustion process becomes an integral part of the industrial combustor design process.

A concept of modeling combustor using chemical reactor such as PSR, PFR and MIX was introduced by S. L. Bragg [1]. Zonal combustion modeling was proposed by Swithenbank as an improvement for combustor design via correlation parameters, and followed experimental testing [2]. In the zonal modeling, the combustor volume is

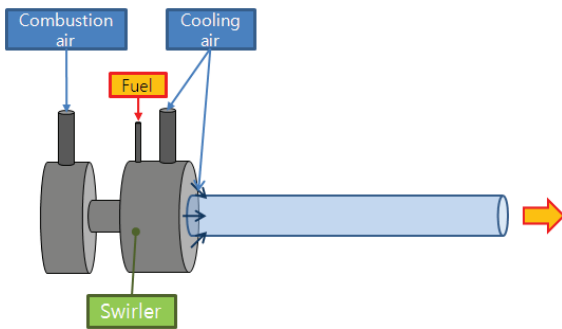
divided into zones represented by idealized reactor elements. Rubins and Pratt applied the zonal model to study emissions control in gas turbine combustion [3]. The chemical reactor modeling of combustion systems are not necessarily limited to the use of extensive chemical reactor networks. Recently, Rutar *et al.* [4], Rutar and Malte [5], Park, J. K. [6, 7], and Lee *et al.* [8] have shown a methodology for modeling the pollutant emissions of the experimental jet stirred reactor with a simple idealized reactor scheme. A hybrid CFD-CRN model for the gas turbine combustors was proposed by Sturgess and Shouse [9]. The post-processing of the CFD simulations was employed for the development of CRN model. Roby *et al.* modeled the experimental results of Mellor by using a CRN with the main combustion zone split into two streams to account for imperfect fuel-air premixing [10, 11]. Novesselov also employed a CRN for emissions prediction of the lean premixed gas turbine combustor [12]. The chemical reactor modeling is found to be a valuable tool in the evaluation of pollutant formation and blow-out the performance of combustion systems. The methodologies of the development vary between authors.

Different methods have been presented in the mechanical literature for modeling the turbulent combustion process. However, there are no computer models available to incorporate the full set of chemical kinetic reactions coupled with turbulent flow modeling. In order to model complex combustions, various simplified global kinetic mechanisms are developed. Even the use of a simplified chemistry in conjunction with CFD for an industrial combustor can take a long time for a combustor designer. An intelligently designed CRN can provide answers regarding the quantitative NO<sub>x</sub> behavior of the industrial combustor. In this work, the CRN approach is applied to predict NO<sub>x</sub>

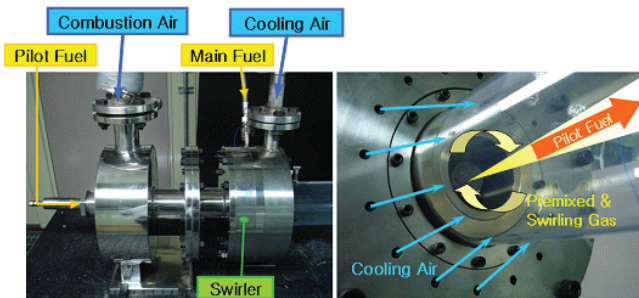
for the industrial combustor. The prediction of NO<sub>x</sub> by the CRN approach is compared with the experimental data for the verification of the model. The effects of equivalence ratio, swirl angle, pilot fuel ratio are investigated.

## II. DESCRIPTION OF MODELS

Figure 1 shows the experiment and the schematic diagram of the combustor which is used in experiment. The model system is composed with a combustor liner and an injector which has a pre-mixer and a pilot. Cooling air is supplied through a hole to impact the combustor liner. For the measurement of emission density, Testo 360 gas analyzer was used. This equipment extracts the emission gas sample. Also, the R-type thermocouple probe, which is possible to use from the room temperature up to 1700K, was used for measuring the combustor exit temperature. The measurement location was from R/2 points of radius direction. The pre-heated air temperature was fixed at 650K and the pressure condition is 1atm. The overall fuel-air equivalence ratio was changed from 0.5 to 0.7. Three different swirl angles of 30°, 45°, and 60° were used. Pilot fuel-air mixture ratio varied from 0 to 10% of the injector flow rate; the rich pilot corresponds to the lower premixed equivalence ratio than the normal one.



(a) Schematic Diagram of Industrial Combustor



(b) Experimental Model of Industrial Combustor  
Fig. 1 Experimental Industrial Combustor Model

CFD modeling provides a basic insight of the flow, the temperature and the species of fields/profiles in the industrial combustor. These fields/profiles aid the visualization, the interpretation of the industrial combustor flow and the reaction space. They are also necessary for constructing an accurate CRN. In this study, the model combustor is modeled by using STAR-CCM software version 4.02, which is a commercial CFD code. For a turbulent model, the k-ε model which has a good convergence is used [7]. Combustion reactions were analyzed with the Eddy Break-Up combustion model.

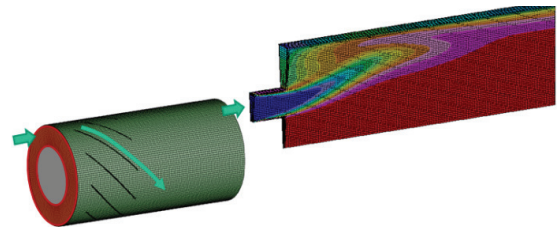


Fig. 2 The Geometry of Swirl Angle and Chamber

The model industrial combustor shown in Figure 2 is a 3D partial model of the swirl angle and the combustor, which was designed by simplifying the experimental combustor for a rapid calculation. The main swirl piece and the injector which has pilot fuel nozzle piece. The combustor used in the actual experiment is more complex, but it is simplified for modeling. A five-million cell, sector geometry with a periodic boundary condition is used. The fuel used in the CFD modeling is assumed as Methane for the actual natural gas used in the engine rig testing.

A representative temperature field in the combustor is shown in Figure 3. This figure shows the zone with a 20% CO concentration compared with its maximum, which assumes the main flame, the zone where the axial velocity is zero, and the temperature field in the combustor at the equivalence ratio 0.6 for three different swirl angles of 30°, 45°, and 60° without a pilot fuel injection. The flame zone was identified with the criteria of 20% of CO concentration (as dotted line in Figure 3), and the other parts as post flame zones. The recirculation zone on the wall surface of the liner is the dome recirculation zone where the temperature distribution is at the lowest due to the forced cooling in the entire combustion zone. The main recirculation zone is the recirculation zone at the center of the combustor, and is highly affected by the swirl at the entrance. Also, Figure 3 shows that the swirl has an effect on the size of the flame zone, the recirculation zone.

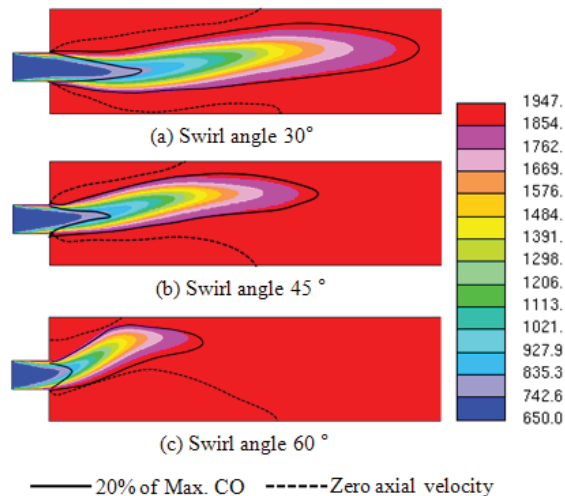


Fig. 3 The Temperature Contours Plot from Star-CCM Software Showing the Presence of the Different Swirl Angles at Equivalence Ratio of 0.6 for Non-Pilot Injection Case

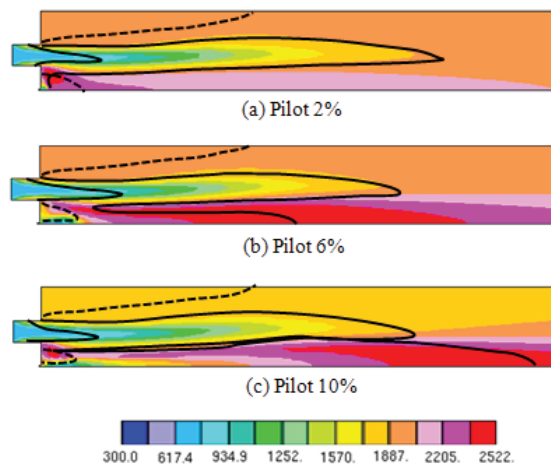


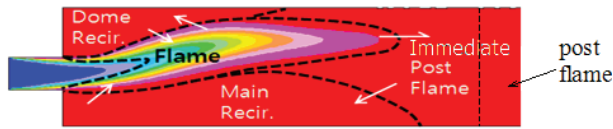
Fig. 4 The Temperature Contours Plot from Star-CCM Software Showing the Presence of the Different Pilots at Equivalence Ratio of 0.6 for Pilot Fuel Injection Case Chemical Reactor Network Modeling

The CFD analysis was also carried out for the combustor with the pilot fuel injection. In this pilot fuel injection case the swirl number is zero in the main fuel entrance, because the swirl is not attached. The calculation was performed for the pilot ratios of 2%, 6%, and 10%. Figure 4 shows the results of the temperature and 20% CO concentration compared with its maximum in case of the equivalence ratio of 0.6 for three different pilot ratios of 2%, 6%, and 10%. The main flame shape is straight and long because the swirl is not used. The temperature in the pilot flame increases as the pilot fuel ratio increases. Although the entire temperature distribution has a similar pattern in all cases, the size of the pilot flame and the main recirculation zone is varied. The length of pilot flame increases abruptly with the increase of the pilot ratio

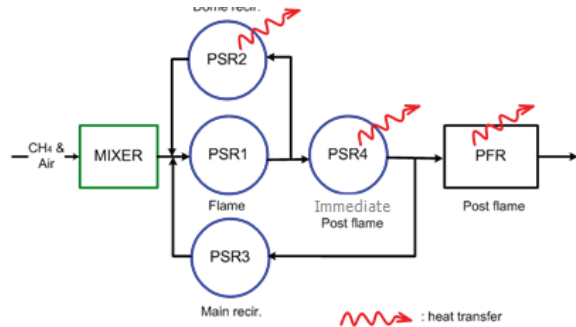
The CRN for the industrial combustor without a pilot fuel injection is developed herein. The chemical reactor code, CHEMKIN software with the detailed chemical kinetic mechanism GRI 3.0 is used for the modeling. The fuel used in the modeling is Methane. The industrial combustor can be divided into zones based on the flow temperature, the velocity, and the chemical species concentrations from the CFD analysis. Figure 5(a) shows the flame shape and location, the entrainment of gas from the dome recirculation zone and the main recirculation zone into the flame, the gas flow from the flame into the dome recirculation zone and the post flame zone, and the gas flow from the post flame zone into the main recirculation zone, etc.

Figure 5(b) shows the layout of the 6-element CRN which is constructed based on the CFD-predicted results. The network consists of one MIX, four PSRs and one PFR elements. PSR is generally defined as a reactor where mixing to the molecular is assumed to happen instantaneously compared to the chemical reaction. The combustion occurs homogeneously in the reactor. A Plug Flow Reactor (PFR) is a reactor where the flow is assumed to move as a plug and the chemical reaction proceeds one-dimensionally, longitudinal mixing in the reactor is assumed to be zero. MIX stands for an element in which the entering streams are uniformly mixed without the chemical reaction. The first element in the CRN arrangement is the MIX, which represents the cone shape zone of the inlet mixture where the mixture is not ignited yet. The flame zone, the dome recirculation zone, the main recirculation zone, and the immediate post flame zone are modeled by using the PSR., while the post flame zones is modeled by using the PFR.

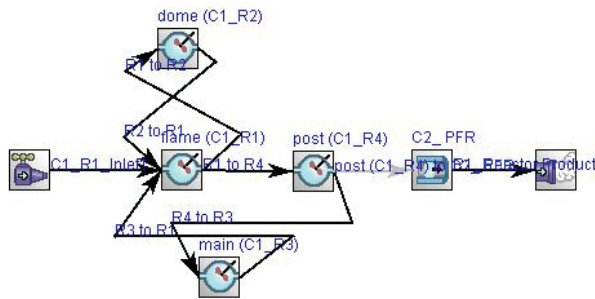
The main flame volume in the CFD simulation can be estimated by calculating the volume confined by iso-CO surface (the value is 20% of the maximum CO concentration). The volume of the dome recirculation zone and the main recirculation zone can be determined from the flow pattern and the temperature field. The volume of the post flame where the flow is assumed to be the plug flow is determined by the flow result. Then, the volume of the immediate post flame is finally determined. The flow splits between the elements in the 6-element CRN are chosen based on the CFD results for the industrial combustor as shown in Figure 5(a). The mass flow rates toward each reactor were calculated at the boundary of each reactor by taking a surface integral of mass flux over the surface. The cooling of the combustion liner is achieved by a convection heat transfer. The averaged heat transfer coefficient is used



(a) The Flame Zone Mapping Based on CFD Result with Swirl Angle of 45° and  $\phi=0.6$



(b) The Schematic Layout of the 6-Element CRN Model



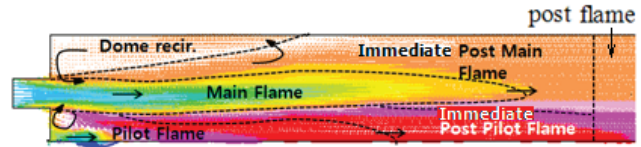
(c) The 6-Element CRN Model for Evaluating the NO<sub>x</sub> Emissions Based on CHEMKIN Software  
Fig. 5 The CRN Modeling for Non-Pilot Injection Case

in this study even though the heat flux varies along the liner. The heat loss in the PSR which contacts with the combustor liner is calculated by using the averaged heat transfer coefficient.

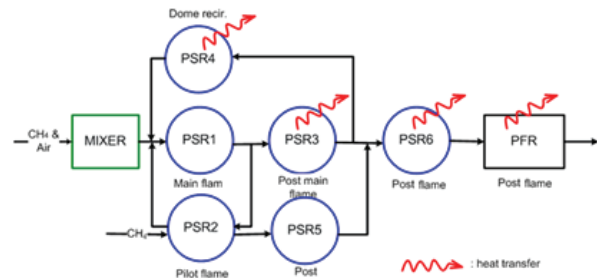
The CRN modeling was also conducted for the industrial combustor with the pilot fuel injection. Figure 6(a) shows the main and the pilot flame shape and location, the entrainment of gas from the dome recirculation zone and the pilot flame zone into the flame, the gas flow from the flame into the immediate post main flame zone and the pilot flame zone, and the gas flow from the post main flame zone into the dome recirculation zone and the post flame, the gas flow from the pilot flame to the immediate post pilot flame zone, and the gas flow from the immediate post main flame zone and the immediate post pilot flame into the post flame zone.

Figure 6(b) shows the layout of the 8-element CRN developed for the industrial combustor with the pilot fuel

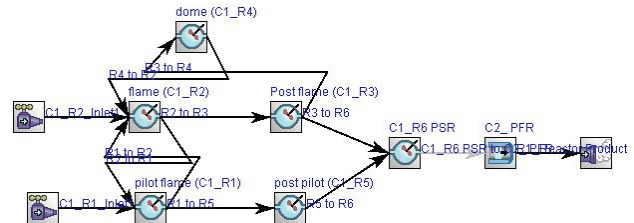
injection. The main flame zone, the recirculation zone and the immediate post flame zone are modeled by using the PSR. The immediate post flame zone is divided into the immediate post main flame zone and the immediate post pilot flame zone because of a big temperature difference.



(a) The Flame Zone Mapping Based on CFD Result with Pilot Fuel Ratio of 6% and  $\Phi=0.6$



(b) The Schematic Layout of the 8-Element CRN model



(c) The 8-Element CRN Model for Evaluating the NO<sub>x</sub> Emissions Based on CHEMKIN Software  
Fig. 6 The CRN Modeling for Pilot Fuel Injection Case

The flow splits between the elements in the 8-element CRN are chosen based on the CFD results for the industrial combustor as shown in Figure 6(a).

### III. RESULTS AND DISCUSSIONS

Figure 7 shows the NO<sub>x</sub> predictions with three different equivalence ratios of 0.5, 0.6, and 0.7 for three different swirl angles of 30°, 45°, and 60° without the pilot fuel injection for Methane as the fuel by using the 6-element CRN as shown in Figure 5, and the comparison of the predicted results to the experimental data for natural gas as fuel. The lines denote the predicted results, and the dots denote the experimental data. The CRN predicted NO<sub>x</sub> emissions results show the reasonably good agreement with the experimental data. Both the CRN predicted results

and the experimental data show that the NO<sub>x</sub> increase as the equivalence ratio increases. The CRN model under-predicted is compared to experimental data when the equivalence ratio is low ( $\phi < 0.6$ ), and over-predicted is compared to the experimental data when the equivalence ratio is high ( $\phi > 0.6$ ). The effects of the swirl angle on the NO<sub>x</sub> emissions is not as strong as the one which can be seen in the Figure 7, but both the CRN predicted results and the experimental data show that the lowest NO<sub>x</sub> emission is found at the swirl angle of 45°, while the higher NO<sub>x</sub> emissions are found at the larger swirl angle of 60°, and the smaller swirl angle of 30°.

Figure 8 shows the mole fraction of NO<sub>x</sub> at each reactor zone for three different equivalence ratios of 0.5, 0.6, and 0.7 at the swirl angle of 30° without the pilot fuel injection. The mole fraction of NO<sub>x</sub> in each of reactor zones (the main flame zone, the main recirculation zone, the dome recirculation zone, and the immediate post flame zone) increases as the equivalence ratio increases, because the temperature in each reactor zone increases with the increase of the equivalence ratio as shown in Figure 9. The temperature in the dome recirculation zone is the lowest among the reactor zones due to the heat transfer in the wall. The increase of mole fraction of NO<sub>x</sub> from the equivalence ratio between 0.6 and 0.7 is much larger than the increase of the mole fraction of NO<sub>x</sub> from the equivalence ratio between 0.5 and 0.6, because the NO<sub>x</sub> formation increases exponentially as the temperature increases.

Figure 10 shows the mole fraction of NO<sub>x</sub> at each reactor zone for the three different equivalence ratios of 0.5, 0.6, and 0.7 at the swirl angle of 45° without the pilot fuel injection and Figure 12 shows the mole fraction of NO<sub>x</sub> at each reactor zone for the three different equivalence ratios of 0.5, 0.6, and 0.7 at the swirl angle of 60° without pilot fuel injection. The mole fraction of the NO<sub>x</sub> distribution in this case is similar to the swirl angle of 30° case.

Figure 14 shows the mole fraction of NO<sub>x</sub> at each reactor zone for the three different swirl angles of 30°, 45°, and 60° at the equivalence ratio of 0.5 without the pilot fuel injection. The smallest mole fraction of the NO<sub>x</sub> emissions is found at the swirl angle of 45°, while the larger mole fraction of

the NO<sub>x</sub> emission is found at the swirl angles of 30°, 60°, because the temperatures in all the reactor zones increase to the higher temperatures at the swirl angles of 30°, 60° as shown in Figure 15. Figure 16 shows the mole fraction of NO<sub>x</sub> at each reactor zone for the three different swirl angles of 30°, 45°, and 60° at the equivalence ratio 0.6 without the pilot fuel injection and Figure 18 shows the mole fraction of NO<sub>x</sub> at each reactor zone for the three different swirl angles of 30°, 45°, and 60° at the equivalence ratio of 0.7 without the pilot fuel injection. The mole fraction of the NO<sub>x</sub> distribution in this case is similar to the equivalence ratio of 0.5.

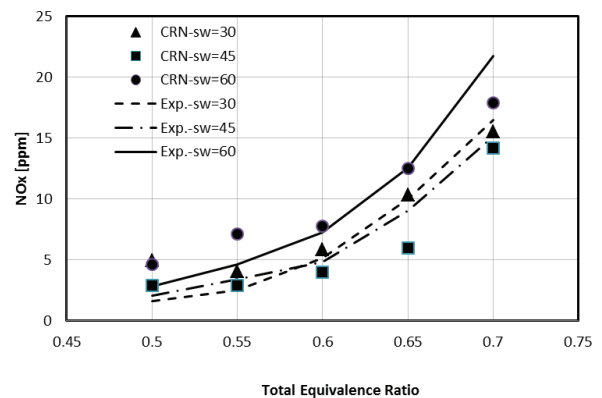


Fig. 7 The Mole Fraction of NO<sub>x</sub> Emissions with Equivalence Ratio for Non-Pilot Injection Case

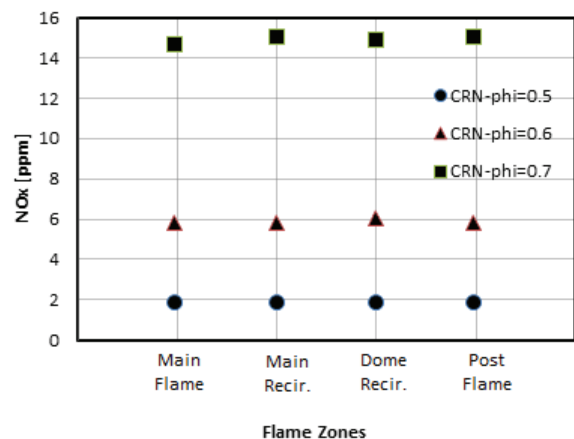


Fig. 8 The Mole Fraction of NO<sub>x</sub> in each Reaction Zone for Non-Pilot Injection Case at Swirl Angle of 30°

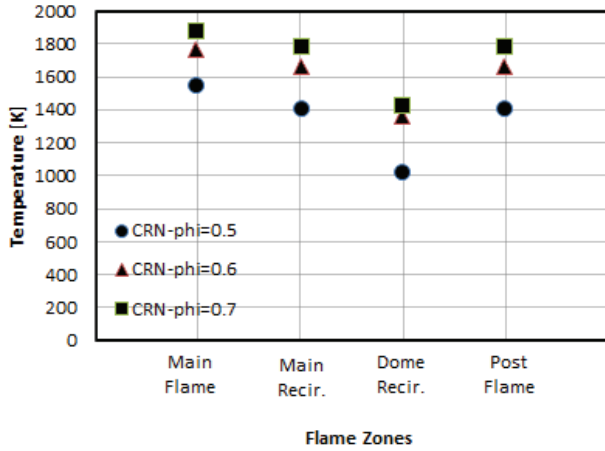


Fig. 9 The Temperature in each Reaction Zone for Non-Pilot Injection Case at Swirl Angle of 30°

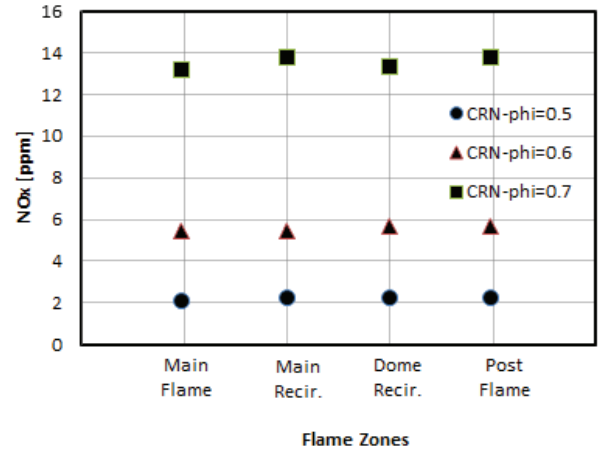


Fig. 12 The Mole Fraction of NOx in each Reaction Zone for Non-Pilot Injection Case at Swirl Angle of 60°

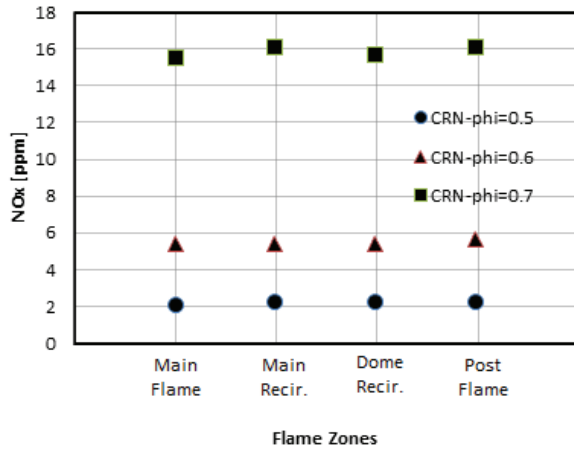


Fig. 10 The Mole Fraction of NOx in each Reaction Zone for Non-Pilot Injection Case at Swirl Angle of 45°

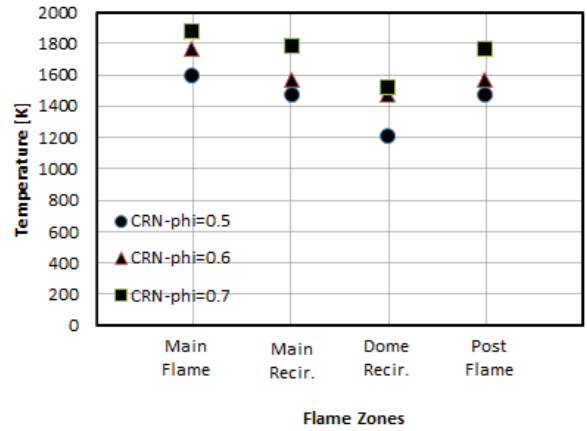


Fig. 13 The Temperature in each Reaction Zone for Non-Pilot Injection Case at Swirl Angle of 60°

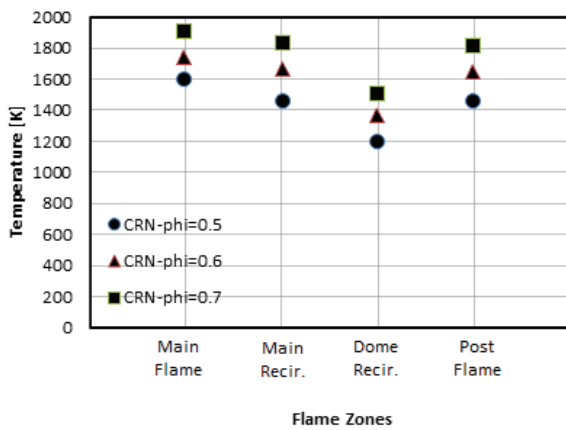


Fig. 11 The Temperature in each Reaction Zone for Non-Pilot Injection Case at Swirl Angle of 45°

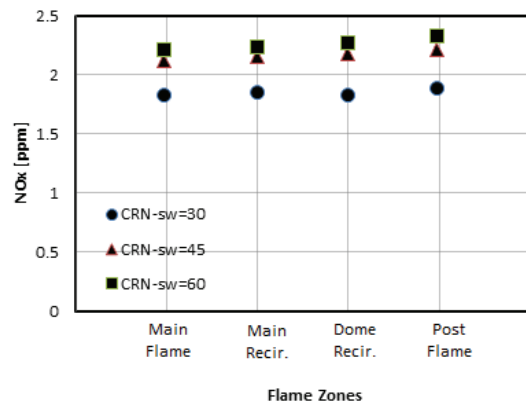


Fig. 14 The Mole Fraction of NOx in each Reaction Zone for Non-Pilot Injection Case at Equivalence Ratio of 0.5

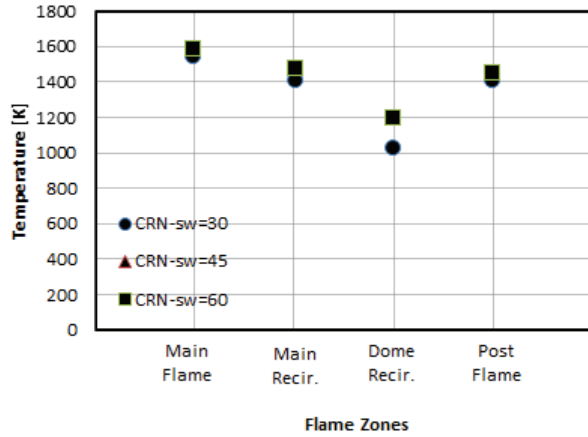


Fig. 15 The Temperature in each Reaction Zone for Non-Pilot Injection Case at Equivalence Ratio of 0.5

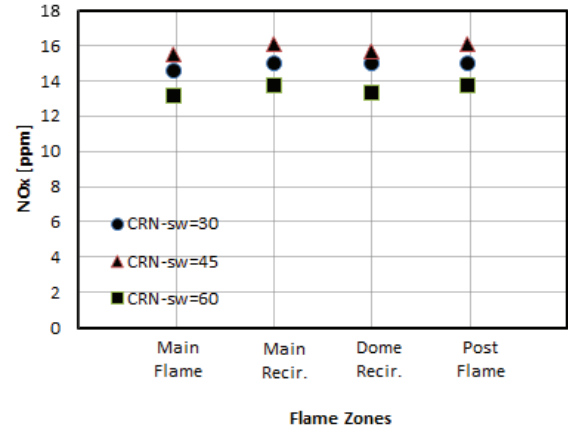


Fig. 18 The Mole Fraction of NOx in each Reaction Zone for Non-Pilot Injection Case at Equivalence Ratio of 0.7

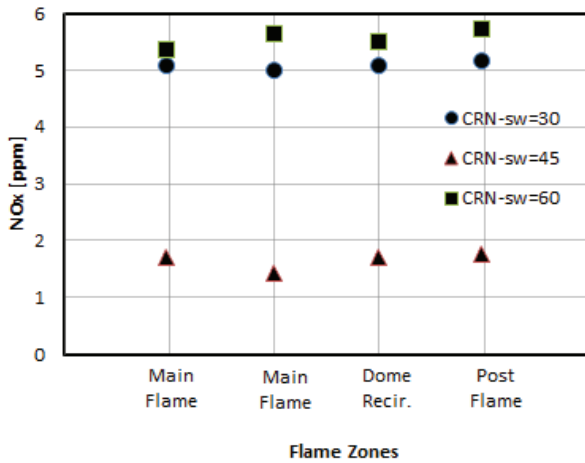


Fig. 16 The Mole Fraction of NOx in each Reaction Zone for Non-Pilot Injection Case at Equivalence Ratio of 0.6

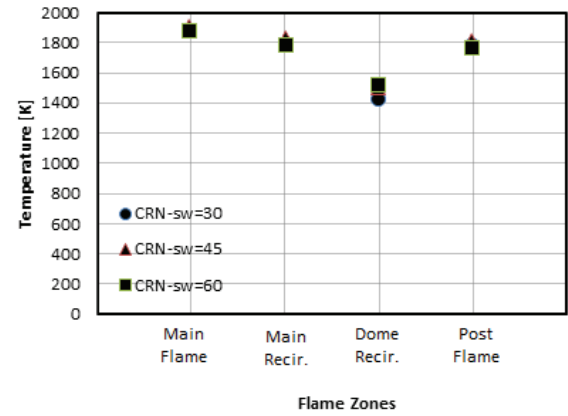


Fig. 19 The Temperature in each Reaction Zone for Non-Pilot Injection Case at Equivalence Ratio of 0.7

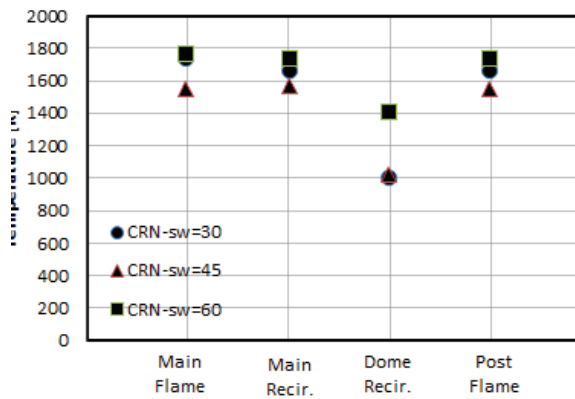


Fig. 17 The Temperature in each Reaction Zone for Non-Pilot Injection Case at Equivalence Ratio of 0.6

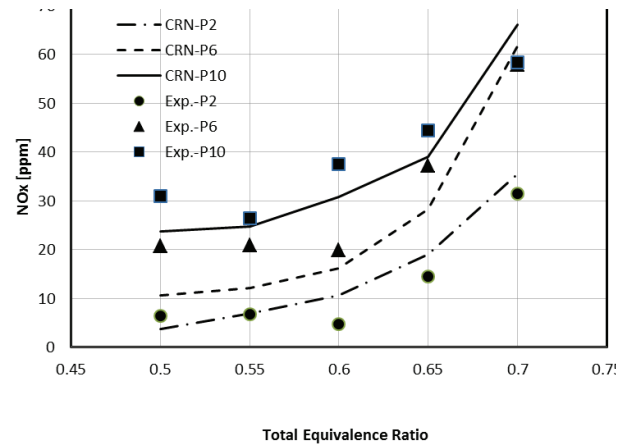


Fig. 20 The Mole Fraction of NOx Emission with Equivalence Ratio for Pilot Fuel Injection Case

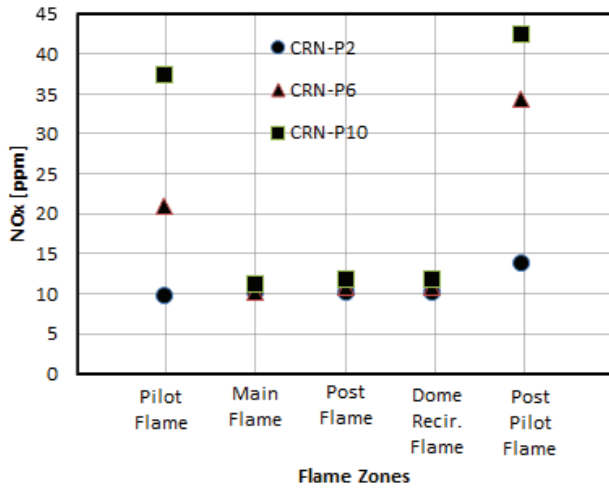


Fig. 21 The Mole Fraction of NO<sub>x</sub> in each Reaction Zone for Pilot Fuel Injection Case at Equivalence Ratio of 0.7

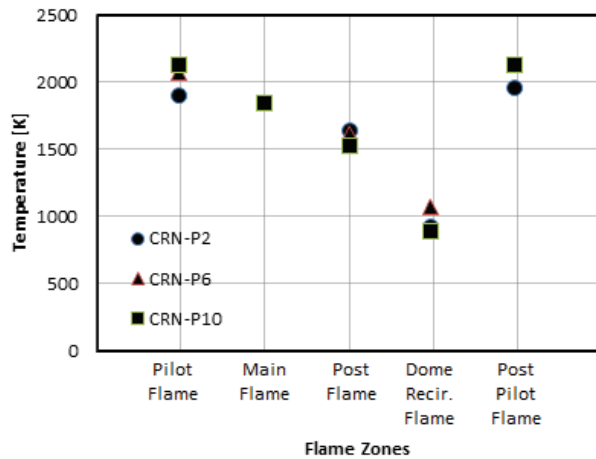


Fig. 22. The Temperature in each Reaction Zone for Pilot Injection Case at Equivalence Ratio of 0.7

Figure 20 shows the NO<sub>x</sub> predictions with the different equivalence ratios of 0.5, 0.6, and 0.7 for the three different pilot fuel ratios of 2%, 6%, and 10% without the swirl by using the 8-element CRN model as shown in Figure 6, and comparison of the predicted results with the experimental data. The predicted results of the NO<sub>x</sub> emission show the reasonably good agreement with the experimental data. Both the CRN predicted results and the experimental data show that the NO<sub>x</sub> increases with increase of the overall equivalence ratio and the pilot fuel ratio.

Figure 21 shows the mole fraction of NO<sub>x</sub> at each of reactor zones (the main flame zone, the pilot flame zone, the immediate post flame zone, the dome recirculation zone, and the immediate post pilot flame zone) for the three different pilot fuel ratios of 2%, 6%, and 10% at

the equivalence ratio of 0.6. When the pilot fuel ratio is small, the mole fraction of NO<sub>x</sub> in each reactor is almost the same except for the post pilot flame zone. However, if the pilot fuel ratio increases, the mole fractions of NO<sub>x</sub> in the pilot flame zone and the post pilot flame zone increase much more than other reactors because the temperature increases to a very high temperature above 2000K as shown in Figure 22. The amount of the NO<sub>x</sub> emissions produced in an industrial combustor is strongly linked to the time that the combustion products spend at high temperatures. In the design of industrial combustor, therefore, the temperature-versus-time relationship for the gas flow may compromise the useful operation of the industrial combustion device.

Figure 22 also shows the fuel-energy specific NO<sub>x</sub> emissions for simple methane-air jet flame. We observe that the characteristic trend with heat release rate varies with zones. These trends are explained by temperature. Thus, we see that for the more luminous flames and the larger flames, temperature effects prevailing, causing an increasing trend of the NO<sub>x</sub> emissions with the heat release.

#### IV. CONCLUSIONS

This research shows that the use of the combined CFD; and CRN approach has ability to accurately predict the NO<sub>x</sub> emissions for the industrial combustion applications. The CRN can be useful in analyzing the formation and the reduction of the NO<sub>x</sub> emissions. The CRN for the industrial combustor consists of two models as shown in Figure 5 and Figure 6. However, the main difficulty in developing such a CRN is obtaining the reliable CFD simulations for the industrial combustor. The CFD simulations shows that even for the overall equivalence ratio locally rich conditions exit in the core of the flame as shown in Figure 3 and Figure 4.

The diagram of the CRN for the case of non-pilot fuel injection is shown less NO<sub>x</sub> emissions than the diagram of the CRN for the case of pilot fuel injection. The CRN developed herein can be used to explore the effects of the zone temperature and the equivalence ratio on the NO<sub>x</sub> emissions. The results of the CRN modeling are presented below:

- The predicted NO<sub>x</sub> emission by CRN model based on CFD agrees reasonably well with experimental data of test combustor.
- The effect of the swirl on the NO<sub>x</sub> emission is not large, but it was found that the NO<sub>x</sub> emission is the lowest at the swirl vane angle of 45°.
- The NO<sub>x</sub> emission increases as the pilot fuel ratio increases due to the increase of temperature at the pilot flame and the post pilot flame zone.

The CRN tool may be used as a means for parametric analyses and design. It shows a very good capability for predicting the NO<sub>x</sub> emissions. The use of the CRN provides a significant insight into the NO<sub>x</sub> formation behavior. The CRN can handle the most complex chemical mechanisms at the relative ease. It can be used as the means for parametric analyses and be conveniently integrated into the combustor design, because of its small computational time requirement. The CRN can also be used for evaluating the truncated and the global chemical mechanisms for the use in CFD.

#### REFERENCES

- [1] S. L. Bragg, "Application reaction rate theory to combustion chamber analysis", aeronautical research council pub. ARC 16170, Ministry of Defense, London, England, pp.1629-1633, 1953.
- [2] J. Swithenbank, Combustion fundamentals. AFOSR 70-2110 TR, 1970.
- [3] P. M. Rubin, and D. T. Pratt, "Zone combustion model development and use: Application to emissions control. *American Society of Mechanical Engineers*", 91-JPGC-FACT-25, 1991.
- [4] T. Ruta, P. C. Malte, and J. C. Kramlich, "Investigation of NO<sub>x</sub> and CO formation in lean premixed, methane-air, high-intensity, confined flames at elevated pressures", *Proc. Combust. Inst.*, Vol.28, pp.2435-2441, 2000.
- [5] T. Rutar, and P. C. Malte, "NO<sub>x</sub> formation in high-pressure jet-stirred reactors with significance to lean-premixed combustion turbines", *ASME Journal of Engineering for Gas Turbines and Power*, Vol.124, pp.776-783, 2002.
- [6] J. K. Park, "Modelling study of the effect of chemical additives on soot precursors reaction", *International Journal of Automotive Technology*, Vol.7, No.4, pp.501-508, 2006.
- [7] Nguyen Thanh Hao, Nguyen Thanh Nam, Jungkyu Park, "A CRN simulation for emission pollutants prediction in lean premixed gas turbine combustor", *Asean Engineering Journal*, vol.1, 2011.
- [8] B. R. A. Lee, "study on NO<sub>x</sub> formation pathway of methane-air lean premixed combustion by using PSR model", *Transaction of KSAE*, Vol.17, No.5, pp.46-52, 2009.
- [9] G. Sturgess, and D. T. Shouse, "A hybrid model for calculating lean blow-outs in practical combustors", *AIAA* pp. 96-3125, 1996.
- [10] A. M. Mellor, Editor. "NO<sub>x</sub> and CO emissions models for gas-fired, lean premixed combustion turbine: Final report", Vanderbilt University, Nashville, TN, 1996.
- [11] R. J. Roby, M. S. Klassen, D. Vashistat, R. Joklik, A. Marshall, High fuel-air ratio (FAR) combustor modeling. Report to Naval Air Warfare Center, 2003.
- [12] I. V. Novoselov, Eight-step global kinetic mechanism of methane oxidation with nitric oxide formation for lean premixed combustion turbines. MSME Thesis, University of Washington, Seattle, WA, 2002.